Peak Torque Evaluation of IPM 150kW for EVs

[1]Bui Minh Dinh, [2]Nguyen Chi Dung

[1]Hanoi University of Science and Technology (HUST)
dinh.buiminh@hust.edu.vn
[2]Hanoi Viettel High Technology (VHT)
dungnc43@viettel.com.vn

Abstract

This paper presents the design optimization procedure of three-phase interior permanent magnet (IPM) synchronous motors with minimum weight, maximum power output for a wide constant-power range. The particular rotor geometry of the IPM motor with several variables and constraints has been implemented by the DoE method. This study is to combine an accurate finite-element analysis with a multiobjective optimization procedure using a new algorithm belonging to the class of controlled random search algorithms. The optimization procedure has been employed to design two IPM motors for EVs. A prototype has been realized and tested. Torque's current characteristic result comparison between simulated and measured performances shows the reliability of the simulation results of the proposed procedure. The proposal motor design is based on both analytical models and special software to determine the magnetic sizes and geometry parameters of stator and rotor. The experimental test and analytical results have been used to evaluate silicon steel material for designs. To maximize efficiency performance, an optimal algorithm program built-in Matlab and FEM has been written and shown in PC interfaces

Keywords: Interior Permanent Magnet Motor-IPM Motor, Finite Element Analysis-FEA.

Introduction

The IPM motors built with magnets placed inside the rotor body are attracting great attention in several variable-speed applications, such as electric vehicles and industrial and domestic appliances, where the most challenging requirement are high efficiency, high torque density, good overload capability, and extended speed range. The performance of IPM machines is significantly affected by the magnet rotor topologies in Chen Peng 2021, Wenliang Zhao 2015. Thus, several Interior Permanent Magnet Synchronous Motor Design Trend are developing different topology rotor designs such as V-shaped from manufacturer Tesla; double V magnet shape from manufacturer China, delta shape from manufacturer AVL, hybrid delta shape based on the V shape from both manufacturer Tesla and manufacturer Nissan; hybrid double V shape from both manufacturer T and manufacturer V. Those design of rotor shape have aimed to maximize efficiency, torque density, overload load capability Chen Peng 2021, Wenliang Zhao 2015, Yang, Y 2017. This study will focus on multi geometry parameters of the rotor design concept with VV magnet arrangement. This study will improve design average torque current characteristic by hybrid rotor shape design and step skewing magnet segment. In this paper, the Torque and power vs current of the IPM step-skew magnet rotor are manufactured to verify by experiment methods.

Electromagnetic Design

The objective of improving the flux-weakening capability of IPM motors received wide interest in literature in Chen Peng 2021. The design was formulated as a constrained multiobjective optimization problem consisting of maximizing the machine efficiency while minimizing its weight in [6]. The method for maximizing performance by modifying the PM quantity was analyzed in Liu, X 2017. The rotor design optimization of IPM motors for wide speed ranges using an FEA-based multiobjective genetic algorithm with three-goal functions (motor torque, torque ripple, and flux-weakening capability were present in Wang, A.; 2011. This paper proposes a design optimization and evaluation procedure of three-phase IPM synchronous motors suitable for wide constant-power region operation to minimize the motor weight and maximize the output power. An analytical program was developed to estimate torque, efficiency value by MATLAB coupling to FEMM into one program as figure 2. The analytical

calculation has used mathematical calculation of torque per amp in d-q or Psi modeling. The program is divided into three main parts: analytical calculation, exporting drawing, and magnetic stimulation. There are also some supporting parts including the material library which is also associated with the FEMM library.

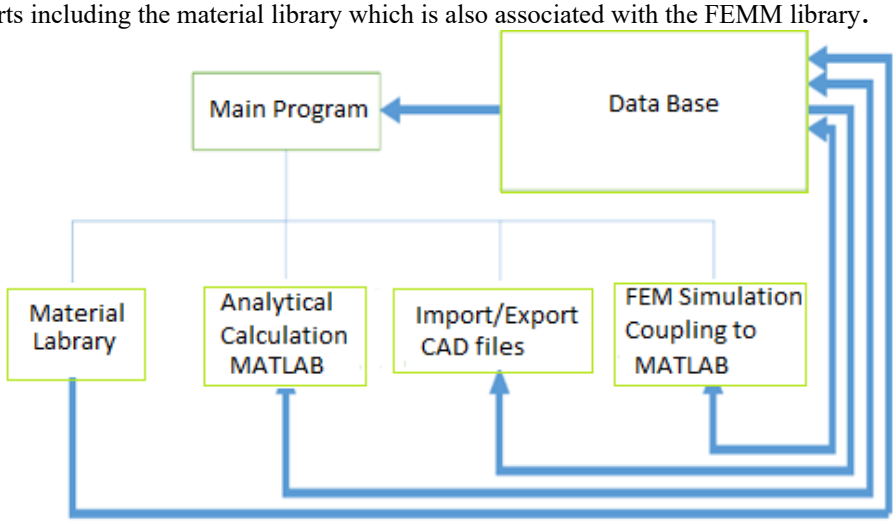

Figure 2. Analytical Program Structure

The electromagnetic torque of an IPM machine is formed from two components of magnetic torque and reluctance torque. The PM component is produced based on the interaction between the air-gap magnetic field and armature reaction magnetic field and the reluctance component is instead on the asymmetry between the PMA-SYNRM machines magnetic circuit of d-axis and-axis. The electromagnetic torque can then be defined as:

$$T\_em = \frac{3.p}{2}\left[\lambda_{pm}.i_d + (L_d - L_q).i_d.i_q\right] \quad (1)$$

The λpm depends on magnet sizes, the q-axis inductance and d-axis inductance for PMA-SYNRM machines are calculated based on rotor magnet barrier and magnet pole V angle. The impact of magnetic saturation on inductance can change Ld & Lq and those values are inconstant, they are varied with d-q axis current I_d and I_q. The d- and q-axis inductances can be calculated as:

$$L_d = \frac{\lambda_d - \lambda_{pm}}{I_d}\Big| \; i_d = 0 \quad (2)$$

$$L_q = \frac{\lambda_q}{I_q}\Big| \; i_q = 0 \quad (3)$$

where λ_{PM} is the flux linkage generated by PM field and λ_d is the d-axis flux linkage generated by armature reaction field between rotor and stator. The FEA-calculated d- and q-axis inductances are shown in Figure 3. The DC link voltage of the power inverter to the PM machine is limited by the maximum bus voltage of batteries. The angular speed of the rotor is limited by the amplitude of the phase voltage. The maximum speed depends on the voltage limitation of the power inverter and d-axis demagnetization current. When the voltage reaches a limited value, it is difficult to further incease the speed as below equation:

$$n_{max} = \frac{U_{lim}}{p(\lambda_{PM} + L_d i_{d\,lim})} \quad (4)$$

To guarantee a wide constant-power operation, the motor requires an accurate design through the use of salient rotor geometry with limited flux contribution from PMs buried within the rotor structure. To achieve the desired degree of saliency, maximize the power density, and guarantee good performance, a special lamination profile should be found. The particular rotor geometry of the IPM synchronous motor and the presence of several variables

and constraints make the design problem very complicated to solve. A good way is to carry out a design procedure, combining accurate FEA with mathematical optimization algorithms. This paper proposes a new design approach based on this idea. The study concerns the design of the following two IPM synchronous motors. The number of slots was 48 and the rated voltage is DC 400 V. The same electrical current was applied to each motor for analysis. The maximum rated current was 600 A. The slot fill factor of 40% or below is known to enable windings, 36.80% was adopted for this design by considering the insulation thickness. The air gap is 0.7 mm and several coils were wound 10 turns to reduce the current density of 15A/mm2.

Figure 5 also provides a cross-sectional view of the 48 slot stator. The outer diameter of an IMP motor stator is 200 mm. To form a sinusoidal back-EMF (B-EMF) at the stator, distributed windings were designed. Because the volume of the magnet is the most influential factor in the production cost and quality of an IPM motor, the magnet volumes for each design are compared in an analytical program to achieve maximum torque per ampere (MTPA) by minimum volume of the motor. The V-shaped rotor had the smallest magnet volume (268.8 mm3), while the delta-shaped rotor from manufacturer N had the largest magnet volume (388.2 mm3). As a small volume motor and high efficiency are critical to EVs, the smallest magnet volume would most likely be the most effective design.

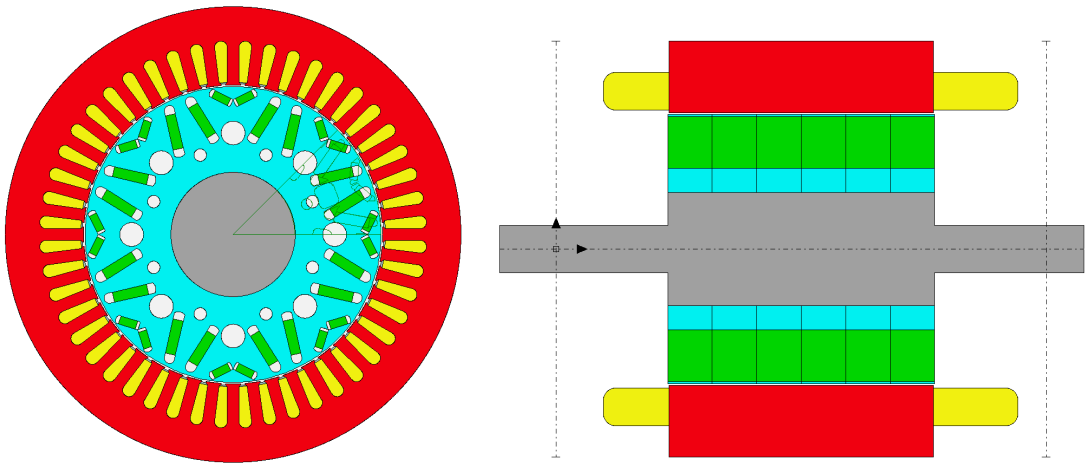

(a) (b)

Figure 1. Motor radial section (a), Six magnet slice of IPM Motors

The limits on the design variables have been chosen to guarantee the feasibility of the final designs. The number of variables and constraints make the optimization problem very complicated and could require significant computational effort. There are five design variables (P1, P2…P5) parametrized diameters as figure 6.

Geometry is optimized at the knee-point with multi-objectives of:

- **Maximize Torque**
- **Minimize Voltage**
- **Minimize Torque ripples**
- **Minimize Radial Force 48th time order – 0 space (T48S0)**

Parameter	Min	Max	Max Torque Variant	Reduced NVH Variant	Trade-off Variant
Lower Magnet Angle (P1)	45	53	49.674	51.328	50.521
Lower Magnet Barrier (P2)	4	5	4.573	4.214	4.327
Upper Magnet Barrier (P3)	0.8	1.2	0.8	0.906	0.951
Upper Magnet Separation (P4)	0.4	0.6	0.469	0.4	0.429
Slot Opening Thickness (P5)	1.8	2.4	2.384	2.322	2.191

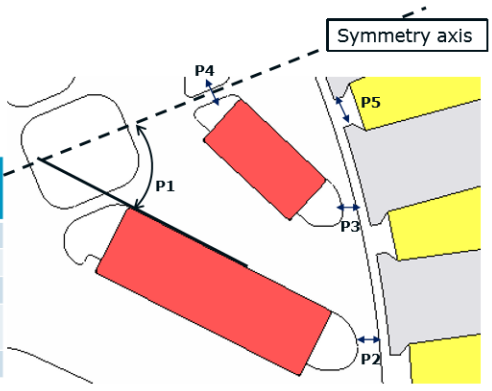

Figure 2. Rotor and stator are parametrized and checked upper and lower boundaries

Design of the Experiment DOE is created and run in FEM. DoE results are used to create behavioral models used for the optimization.

Optimization Algothirm

The optimal design problem of an IPM synchronous motor can be formulated as a particular multi-objective mixed-integer nonlinear programming problem. This study focuses on defining an algorithm that efficiently tackles the mixed-integer aspect of the problem since it appears to be crucial for the considered design problem. With regards to the multiobjective aspect of the optimization problem, the analytic model recommends that for this particular optimal design problem, a good compromise among different objectives can be obtained just by minimizing the sum of the weight of the motor and the opposites of the two torques. Therefore, the general structure of the considered optimization problem is as follows:

$$\begin{aligned} & \min f(x) \\ \text{s.t.} \quad & g(x) \leq 0 \\ & l \leq x \leq u \\ & x_i \in Z, \quad i \in I_z \end{aligned} \tag{5}$$

where Z is the set of their integer numbers:

$$R^n \to R^m, l, u \in R^n, l_i, u_i \in Z, \text{and } i \in I_z. \tag{6}$$

the nonlinearly constrained problem is converted into a box-constrained one by adding to the objective functionaterm which penalizes the nonlinear constraint violations, the objective function is as follow:

$$P(x) = f(x) + \frac{1}{\varepsilon} \max \{0, g_1(x), \ldots, g_m(x)\} \tag{7}$$

where ε = 10-2 is the penalty parameter, the following mixed-integer box-constrained problem is considered:

$$\begin{aligned} & \min P(x) \\ \text{s.t.} \quad & l \leq x \leq u \\ & x_i \in Z, \; i \in I_z. \end{aligned} \tag{8}$$

To solve problem (8) efficiently, a new algorithm belonging to the class of CRS algorithms has been proposed. This class derives from the original algorithm described. Finally, we note that the proposed algorithm does not need a (feasible) starting point. It produces a sequence Sk of sets of points starting from an initial set S0. The points of S0 are usually chosen at random on the set l ≤ x ≤ u. However, if one or more interesting points are known, the algorithm can exploit this information by including these points in the initial set S0. The quality of building modeling of the DoE graph shows the quality of building modeling of DoE responses. The program has been also applied RNN (Recurrent neural network) and/or FreePoly Model for the response behavior

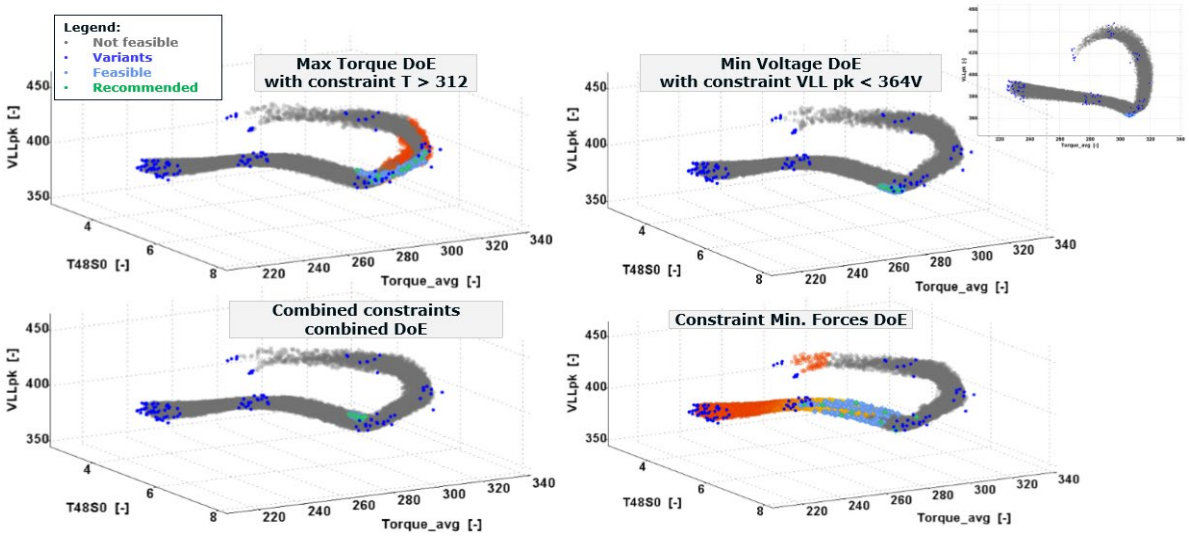

Figure 3. Multi objectives DoE variants

Based on three constraints Max Torque with constraint T > 312, min Voltage with constraint VLL pk < 364V and minimize Radial Forces, the 3D plot of the combined DoE recommended green areas are optimized geometry parameters. From DoE results, efficiency maps of DoE of Baseline, max torque, and Reduced NVH have been shown in figure 10.

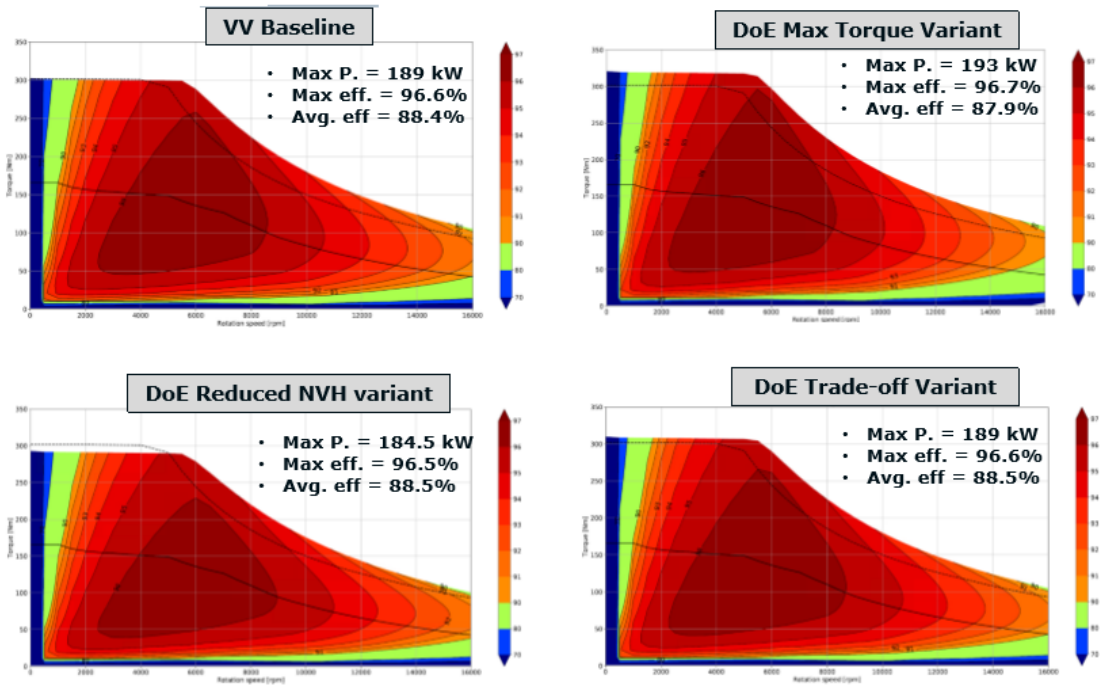

Figure 4. Efficiency maps of Optimized VV variants with nominal rating @490A,400Vdc,100^{0}C

The proposed approach has been employed for the design optimization of IPM synchronous motors to maximize the torque at the base and high speeds, extend the flux weakening region, minimize the motor weight, and satisfy a set of constraints. No initial feasible designs were requested because the optimization procedure does not need to start from a known initial design. Optimized parameters of the IPM motor are shown in table 1.

Table 1. Optimized Parameters of IPM motor

Slot Number	48	L1 Magnet Thickness	3.92	L2 Magnet Thickness	5	Banding Thickness	0
Stator Lam Dia	220	L1 Magnet V Width	10.8	L2 Magnet V Width	22	Shaft Dia	60
Stator Bore	144.2	L1 Magnet Shift	0	L2 Magnet Shift	0.5	Shaft Hole Diameter	0
Tooth Width	5.67	L1 Magnet Bar Width	8.5	L2 Magnet Bar Width	17	Rotor Duct Layers	2
Slot Depth	21.4	L1 Bridge Thickness	0.6	L2 Bridge Thickness	1.7	L1 RDuct Rad Dia	98
Slot Corner Radius	3	L1 Pole V Angle	124.8	L2 Pole V Angle	64	L1 RDuct Channel	8
Tooth Tip Depth	0.7	L1 Outer Extension	0.8	L2 Outer Extension	2.5	L1 RDuct Dia	11.5
Slot Opening	2.1	L1 Inner Extension	0.2	L2 Inner Extension	1	L1 RDuct Angle	0
Tooth Tip Angle	40	L1 Magnet Post	0.1	L2 Magnet Post	13.5	L2 RDuct Rad Dia	83
Sleeve Thickness	0	L1 Magnet Segments	1	L2 Magnet Segments	1	L2 RDuct Channel	8
Pole Number	8	L1 Magnet Clearance	0	L2 Magnet Clearance	0	L2 RDuct Dia	6
Notch Depth	0	L1 Layer Offset Angle	0	L2 Layer Offset Angle	0	L2 RDuct Angle	22.5
Magnet Layers	2			Airgap	0.7		

Peak performance curve

The IPM motor has been manufactured and assembled to set up the test bench. Several functional electrical tests aim is to determine toque, power, voltage, current, and losses. The purpose of the resistance test is to evaluate torque, power, and efficiency vs speed under peak torque and short overload conditions. The test procedure is included several steps such as; calibrating a voltage response concerning rotor temperature for an incoming sample, the rotor response to temperature can be determined so that rotor temperature can be evaluated later by further measurement of the back EMF. Continuous load operating range is setting for testbed dyno at a specified rotor speed range from 2000rpm, 4000rpm, … to 16000rpm, step by step. The experiment test is hold each operating point so that the respective torque and the speed are kept without drift for at least 10 seconds. Finally, the mechanical power is measured and record.

The Peak Performance Testing has been carried out with DC-link Voltage @ 350VDC @400VDC @450VDC to evaluate the maximum torque/ speed curve for peak performance operation at specific boundary conditions.

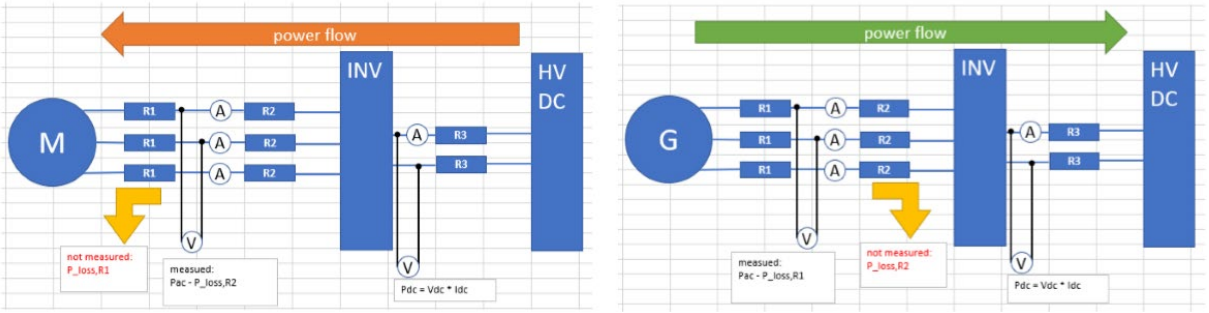

Figure 5. Test bench of IPM system for Q1&4

The IPM is under testing with the measure in Q1 area and electric load will operate as a generator in Q4. Inverter overheating at max output torque in less than 5 s was observed. Motor derating was triggered as inverter temperature reached 95 °C. A particular inverter unit is probably defect . 150 kW output power target was reached only at 400VDC and 450VDC ▪ 300 Nm motor shaft torque target was barely reached at any DC voltage level

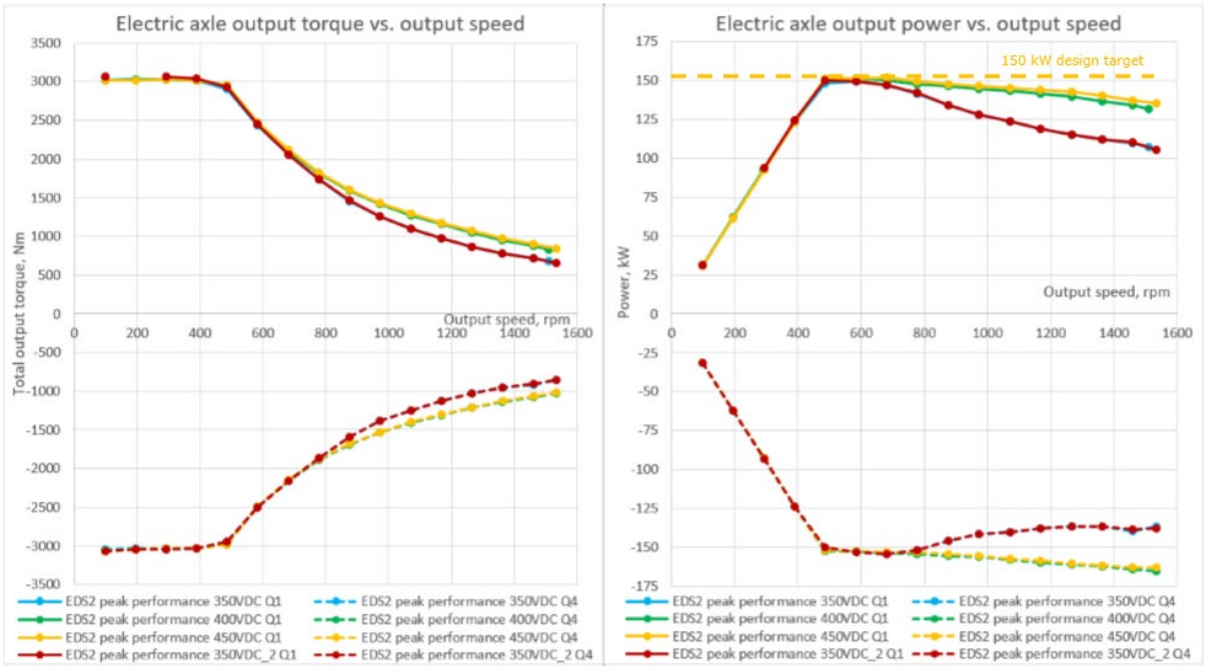

Figure 6 Torque and Power vs speed curves

The corner point is located between measurement points (4000 and 5000 rpm motor speed in driving mode), and therefore can be just estimated by calculations ▪ Corner speed not significantly changing, when DC voltage is varied between 350V and 450V. Output power at high speeds increases intensively between 350VDC and 400VDC. No degradation was observed during aftertest measurement at 350VDC (red curves). The results are matching initial measurements at 350VDC (blue curves) ▪ One measurement point (350VDC_2, Q1, 2000 rpm) was missed due to test bed issue ▪ 150kW peak output power target was reached only at 400VDC and 450VDC

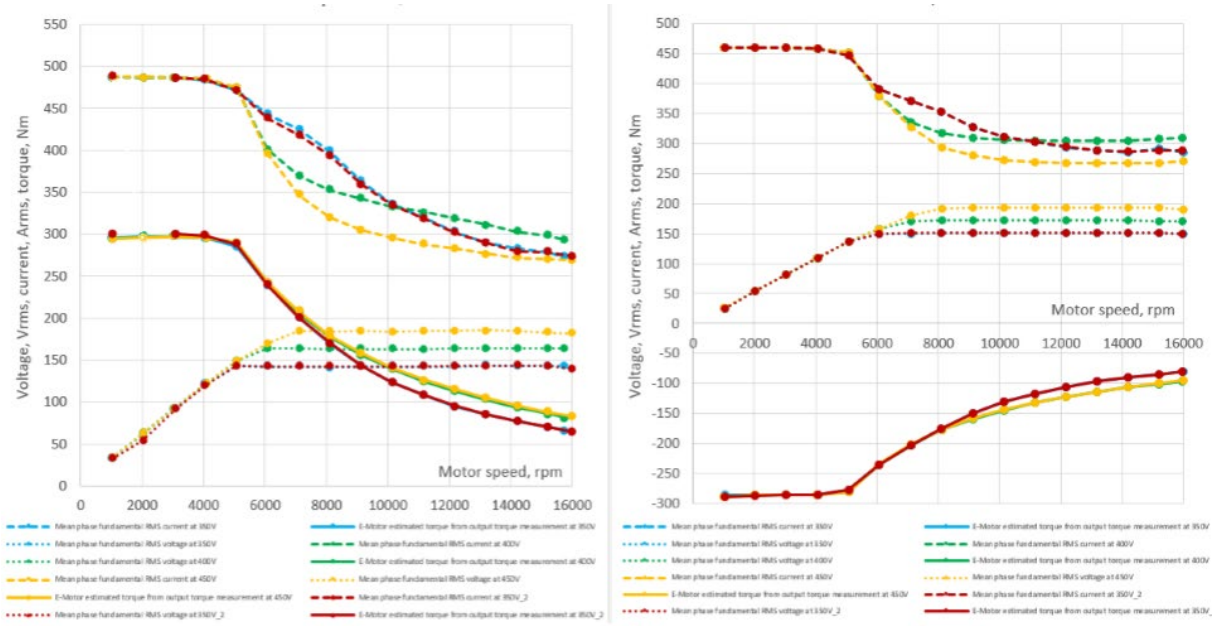

Figure 7 Voltage, current, and torque vs speed curves

From these results in figure 7, it can see that AC current drops above the corner point. There is no change of base speed is observed in the voltage range of 350..450VDC Motor phase current is also approximately 6% higher.

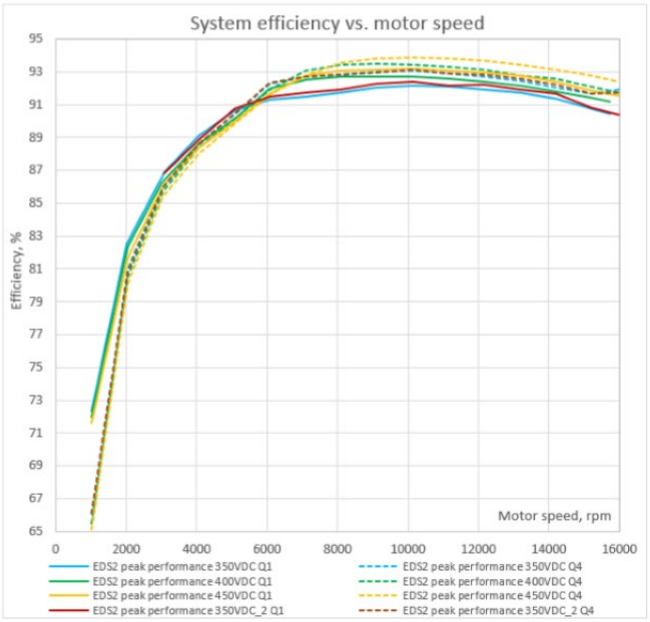

Figure 8 Efficiency curve vs speed with different voltage

Figure 8 shows system efficiency increases along with DC voltage. Max values are 93,2% in driving and 93,9% in braking mode. The regenerative braking mode system efficiency is generally around 1% higher than in driving mode. Because the eAxle is not capable to deliver max torque of 3000 Nm below base speed for 5 s at 450 VDC and the stator starting temperature at starting of the max load is about 72 °C, inverter temperature is 88..90 °C. Available motor torque is cut as soon as inverter temperature reaches 94..95 °C. The TempAlarm_FWD flag is set to "1". Actual load duration (seconds) and inverter temperature rise rate (°C per second) at problematic points are plotted on the chart (left). In general, temperature rise rate increases along with DC voltage. This can be explained by higher switching losses at elevated voltage level

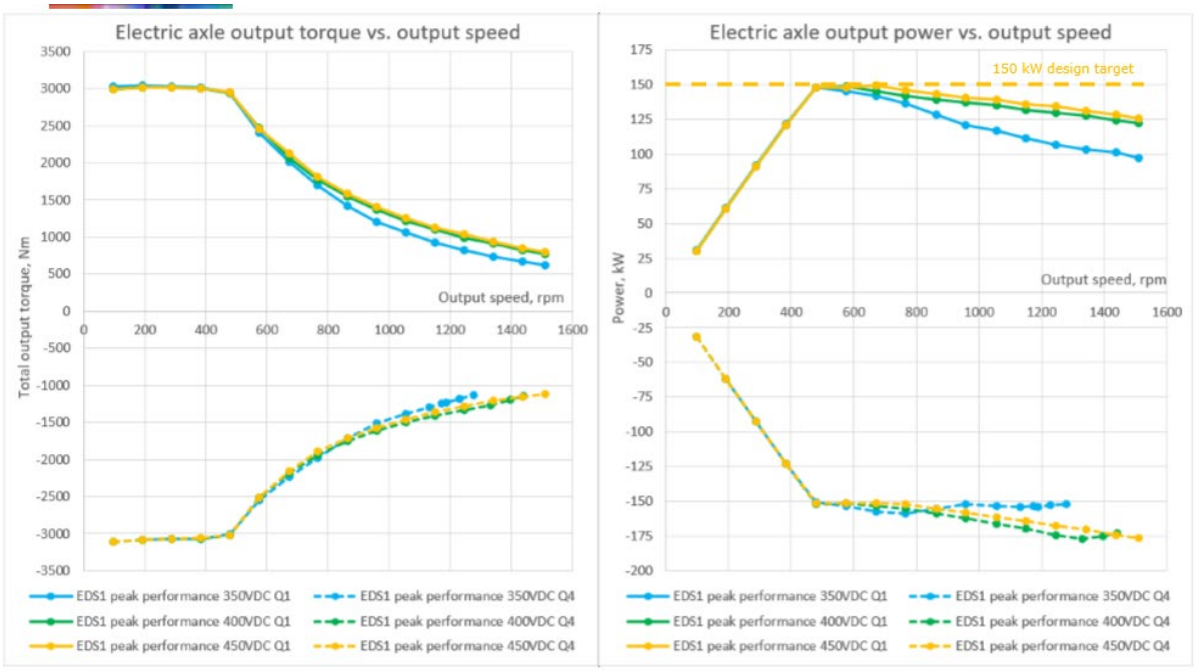

Figure 9 Torque and Power in Short overload

The corner point is located between measurement points (4000 and 5000 rpm motor speed in driving mode), and therefore can be just estimated by calculations ▪ Corner speed not significantly changing, when DC voltage is varied between 350V and 450V. Output power at high speeds increases intensively between 350VDC and 400VDC. Some high-speed points at 350VDC and 400 VDC in regenerative braking mode were not measured due to testbed issues. Power curves in Q1 and Q4 beyond base speed are not symmetric, mainly due to transmission losses. 150kW peak output power target was not reached

Conclusions

This paper has analyzed and compared the DoE optimization of the step-skew IPM motor for EV applications. To verify the proposed design, The Optimized VV variants of a 3-phase 48-slot and 8-pole I PM machine is manufactured and tested. The torque, power, and efficiency under peak torque performance and short overload have been measured at a maximum speed of 16000 rpm. A significant contribution of this study is to figure out DoE result and commends of, max torque, and testing procedures of IPM motor which is useful for developing IPM motor for EV applications. The optimized results and tested performance are good agreement.

REFERENCES

Chen Peng;Daohan Wang;Zhenkang Feng;Bingdong Wang, *"A New Segmented Rotor to Mitigate Torque Ripple and Electromagnetic Vibration of Interior Permanent Magnet Machine"* IEEE Transactions on Industrial Electronics, Year: 2021 | Early Access Article | Publisher: IEEE

Wenliang Zhao;Thomas A. Lipo;Byung-Il Kwon*," Torque Pulsation Minimization in Spoke-type Interior Permanent Magnet Motors With Skewing and Sinusoidal Permanent Magnet Configurations"*, IEEE Transactions on Magnetics Year: 2015 | Volume: 51, Issue: 11 | Journal Article | Publisher: IEEE.

Wenliang Zhao;Thomas A. Lipo;Byung-Il Kwon, *"Torque Pulsation Minimization in Spoke-type Interior Permanent Magnet Motors With Skewing and Sinusoidal Permanent Magnet Configurations"* Year: 2015 | Volume: 51, Issue: 11 | Journal Article | Publisher: IEEE

M. Barcaro, N. Bianchi, and F. Magnussen, *"Design considerations to maximize the performance of an IPM motor for a wide flux-weakening region,"* in Proc. ICEM, 2010, pp. 1–7.

G. Pellegrino and F. Cupertino, "IPM motor rotor design using FEA-based multi-objective optimization," in Proc. IEEE ISIE, 2010, pp. 1340–1346. [23] G. Liuzzi, S. Lucidi, F. Parasiliti, and M. Villani, "Multi-objective optimization techniques for the design of induction motors," IEEE Trans. Magn., vol. 39, no. 3, pp. 1261–1264, May 2003.

W. L. Soong, S. Han, and T. M. Jahns, *"Design of interior PM machine for field-weakening applications,"* in Proc. Int. Conf. Elect. Mach. Syst., Oct. 8–11, 2007, pp. 654–664. Kioumarsi, A.; Moallem, M.; Fahimi, B. Mitigation of Torque Ripple in Interior Permanent Magnet Motors by Optimal Shape Design. IEEE Trans. Magn. 2006, 42, 3708–3710. [CrossRef]

Yang, Y.; Castano, S.; Yang, R.; Kasprzak, M.; Bilgin, B.; Sathyan, A.; Dadkhah, H.; Emadi, A. "*Design and Comparison of Interior Permanent Magnet Motor Topologies for Traction Application"*. IEEE Trans. Transp. Electrify. 2017, 3, 4–9

Liu, X.; Lin, Q.; Fu, W. *"Optimal Design of Permanent Magnet Arrangement in Synchronous Motors".* Energies 2017, 10, 1700.

Wang, A.; Jia, Y.; Soong, W.L. "*Comparison of Five Topologies for an Interior Permanent-Magnet Machine for a Hybrid Electric Vehicle"*. IEEE Trans. Magn. 2011, 47, 3606–3609.

Bui Minh Dinh is a Lecturer and researcher at Hanoi University of Science and Technology in Vietnam. He received a Ph.D. in Electric Motor Design and Manufacture in 2014 at the Technical University of Berlin, Germany, Among his research interests there are high-speed motor design and manufacture related to industrial products such as SRM, IPM, and IM motors. He has managed Viettel R&D for IDME design and Electromagnetic Advisor for Hanoi Electromechanic Manufacturer. Since 2019 he has been a technical advisor for several Electrical Vehicle Companies in Vietnam Such as M1 Viettel, Selex Motor Abaco, and Vinfast